



GPO PRICE \$ _____

CFSTI PRICE(S) \$ _____

Hard copy (HC) \$3.00

Microfiche (MF) 1.65

653 July 65

Fourth Quarterly Report

STUDY PROGRAM ON
(30 - 100 GHz) ELECTRONICALLY STEERABLE ANTENNA SYSTEMS

20 April 1967 - 20 July 1967

Contract NAS 5-10256

Prepared for

Communications Research Branch
Goddard Space Flight Center
Greenbelt, Maryland

FACILITY FORM 602

N68-13044
(ACCESSION NUMBER)

37
(PAGES)

CP-91383
(NASA CR OR TMX OR AD NUMBER)

(THRU) /
(CODE) 07
(CATEGORY)

ADVANCED TECHNOLOGY CORPORATION

1830 YORK ROAD

TIMONIUM, MARYLAND

Fourth Quarterly Report
STUDY PROGRAM ON
(30 - 100 GHz) ELECTRONICALLY STEERABLE ANTENNA SYSTEMS

20 April 1967 - 20 July 1967

Contract NAS 5-10256

Prepared by

John M. Cotton, Jr.

ADVANCED TECHNOLOGY CORPORATION
1830 York Road
Timonium, Maryland
21093

for

Communications Research Branch
Goddard Space Flight Center
Greenbelt, Maryland

TABLE OF CONTENTS

	<u>Page</u>
1. INTRODUCTION	1
2. ANTENNA OUTPUT ARRAY	2
2.1 <u>Computed Far Field Patterns</u>	2
2.2 <u>Element Design and Fabrication</u>	8
2.3 <u>Preliminary Test Results</u>	11
3. FEED SYSTEMS	22
3.1 <u>Series Feed</u>	22
3.2 Optical Feed System	24
4. PHASE SHIFTERS	25
5. VARACTOR MULTIPLIERS	27
6. NEW TECHNOLOGY	32
7. PROGRAM FOR THE NEXT INTERVAL	33

LIST OF ILLUSTRATIONS

<u>Figure</u>	<u>Title</u>	<u>Page</u>
1	Electric Field Calculated With Variation in the Amplitude Term, $\theta = 0^\circ$	4
2	Electric Field Calculated With Variation in the Amplitude Term, $\theta = 10^\circ$	5
3	Electric Field Calculated Without Variation in the Amplitude Term, $\theta = 10^\circ$	6
4	Horn Pattern Test Fixture	10
5	Array Factor for Two Elements on $16 \frac{\lambda}{7}$ Centers	13
6	Array Factor for Three Elements on $16 \frac{\lambda}{7}$ Centers	14
7	Single Element Pattern, E-Plane, Hori- zontal Polarization	15
8	Computed Pattern; Two Elements Phased on Boresight E-Plane, Horizontal Polarization	17
9	Measured Pattern; Two Elements Phased on Boresight E-Plane, Horizontal Polarization	18
10	Computed Pattern; Two Elements Phased 10° off Boresight; E-Plane, Horizontal Polarization	19
11	Measured Pattern; Two Elements Phased 10° off Boresight; E-Plane Horizontal Polarization	20
12	Leaky Mitered Bend	23
13	Phase Difference in Output of Two Multipliers	29
14	Efficiency Characteristics of Two Multipliers	30

1. INTRODUCTION

Earlier quarterly reports on this program have summarized studies made to determine the optimum phased array antenna techniques for use at millimeter wavelengths. The specific application is to be a satellite borne electronically steerable antenna. The early work presented a comprehensive survey of the techniques available. The study then continued with a weeding out process which reduced the number of recommended approaches to six. Five of the six employ phase shifting the r. f. either at the transmitting frequency, or at the sub-harmonic, while the sixth uses retrodirective techniques accomplishing the phase shifting at IF.

Of the six, three were selected for further study including actual design and experimental development of a feasibility model at 35 GHz. These three have a common radiating aperture - an array which remains filled, but in the light of the limited steering requirements can employ a smaller number of higher gain elements.

This report summarizes the results of the experimental work done in this quarter on various components of the antenna system. Some of the individual antenna elements have been fabricated and investigations made of possible mutual coupling effects. The component parts of a compact series feed arrangement have been tested and the complete design established. Work has also been done on the phase transfer characteristics of varactor harmonic generators to determine the problems involved with phase control at the sub-harmonic of the transmitter frequency.

2. ANTENNA OUTPUT ARRAY

2.1 Computed Far Field Patterns

During the past quarter, exact computer solutions have been obtained for the far field pattern of the antenna array. The computations were based on the use of a 7 x 7 matrix of square pyramidal horns completely filling a 16λ square aperture. The formulation took into account the phase front curvature across each element, and the amplitude variation across each element in the H-plane case. The necessary integrals can then be written as

$$I_j = \int_{a_j}^{b_j} \cos\left(\frac{7\pi}{16} z\right) \exp\left\{2\pi i \left[\left(\frac{a_j + b_j}{z}\right) \sin \theta + z \sin \phi - \frac{49\pi}{256} \left(z - \frac{a_j + b_j}{2}\right)^2 \right]\right\} dz$$

where

$$a_j = \frac{16}{7} (j - 1) - 8$$

$$b_j = \frac{16}{7} j - 8$$

ϕ = viewing angle measured from boresight.

θ = steering angle measured from boresight.

The field strength in the far field pattern can then be obtained from the summation $\sum_{j=1}^7 c_j I_j$ where the c_j 's are the appropriate weighting factors for the amplitude taper desired across the array.

These integrals have now been evaluated for two values of the parabolic phase - a half radian and a full radian variation. At 35 GHz for the 16λ total aperture, and 7 element array, the half radian case corresponds to a horn whose axial length is 2.174". The

full radian variation would correspond to a horn of 1.057" axial length.

The patterns for these two cases were calculated both for the H-plane case where the electric field amplitude at each horn edge must go to zero, and the E-plane where the amplitude across the horn is uniform. In each of these cases, the pattern was obtained for steering angles of 0° , 2° , 4° , 6° , 8° , and 10° . Plotting of the data is rather tedious, and an analysis of the numerical results can show that the changes from one pattern to the next are quite small. Some of the extreme cases have been plotted, however, and three are included here.

Figure 1 shows the H-plane pattern for the case of a $1/2$ radian variation in the phase front, i. e. the longer horn. The region of primary interest is of course from -12° to $+12^\circ$ for the synchronous orbit case with allowance for errors of positioning in the satellite. This plot is for the 10 dB illumination taper across the aperture. The grating lobe appears properly at 26° and well removed from the region of interest.

Figure 2 presents the same case steered 10° off boresight. The main beam has deteriorated about $1-1/4$ dB. The grating lobe to the opposite side of boresight is now enhanced by the element pattern, but in the angular region of interest is still down some 15 dB.

For the opposite polarity the unsteered beam is, for all practical purposes, the same as Figure 1. In the extreme steering condition, some obvious differences occur in the far sidelobe pattern (See Figure 3). In the region of interest, however, the patterns can be almost exactly overlaid.

As one type of check on the accuracy of the computer program, a third data run was made with the quadratic phase term set to zero. In this form the integrals can be (and have been)

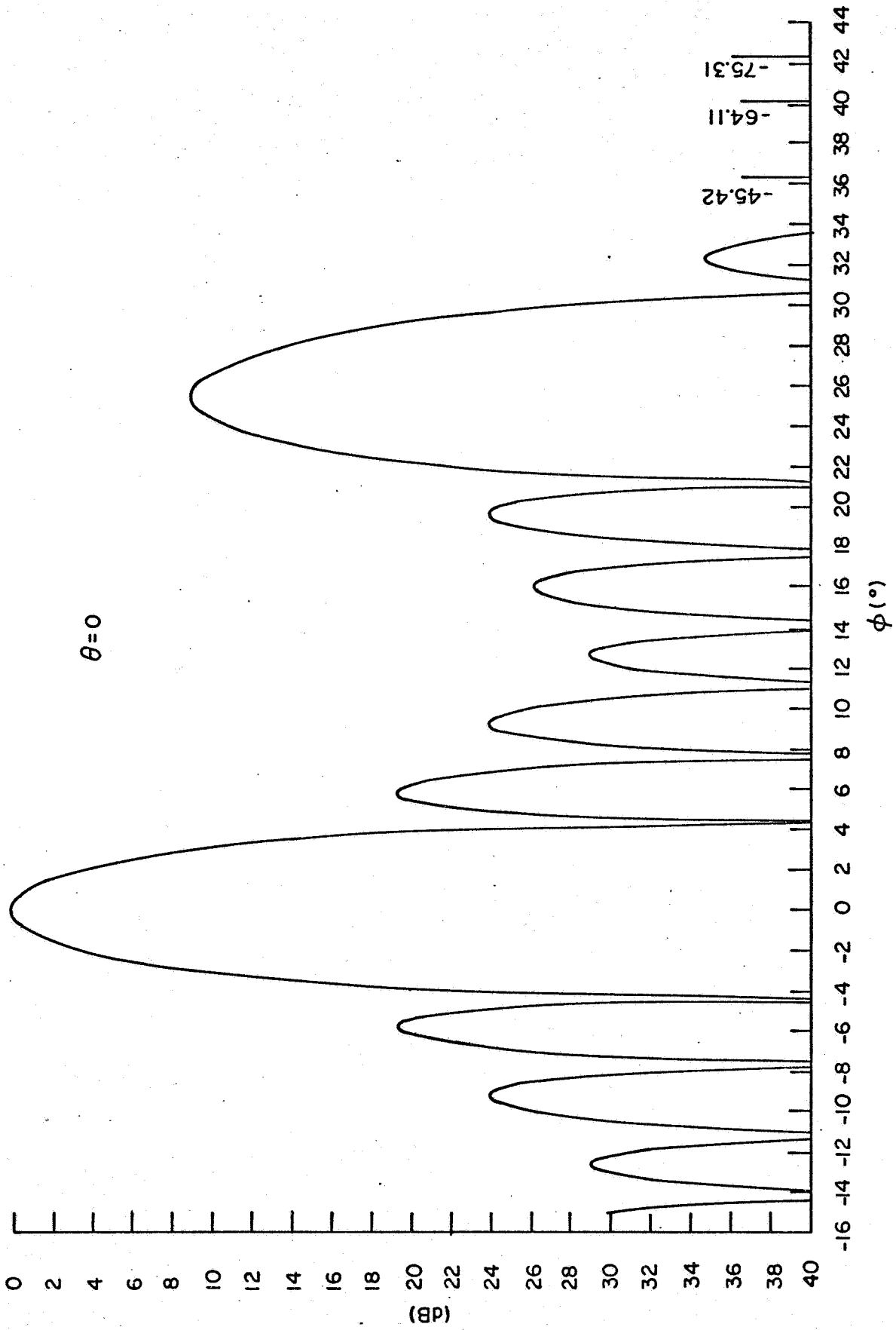


FIG. 1 - ELECTRIC FIELD CALCULATED WITH VARIATION IN AMPLITUDE TERM.

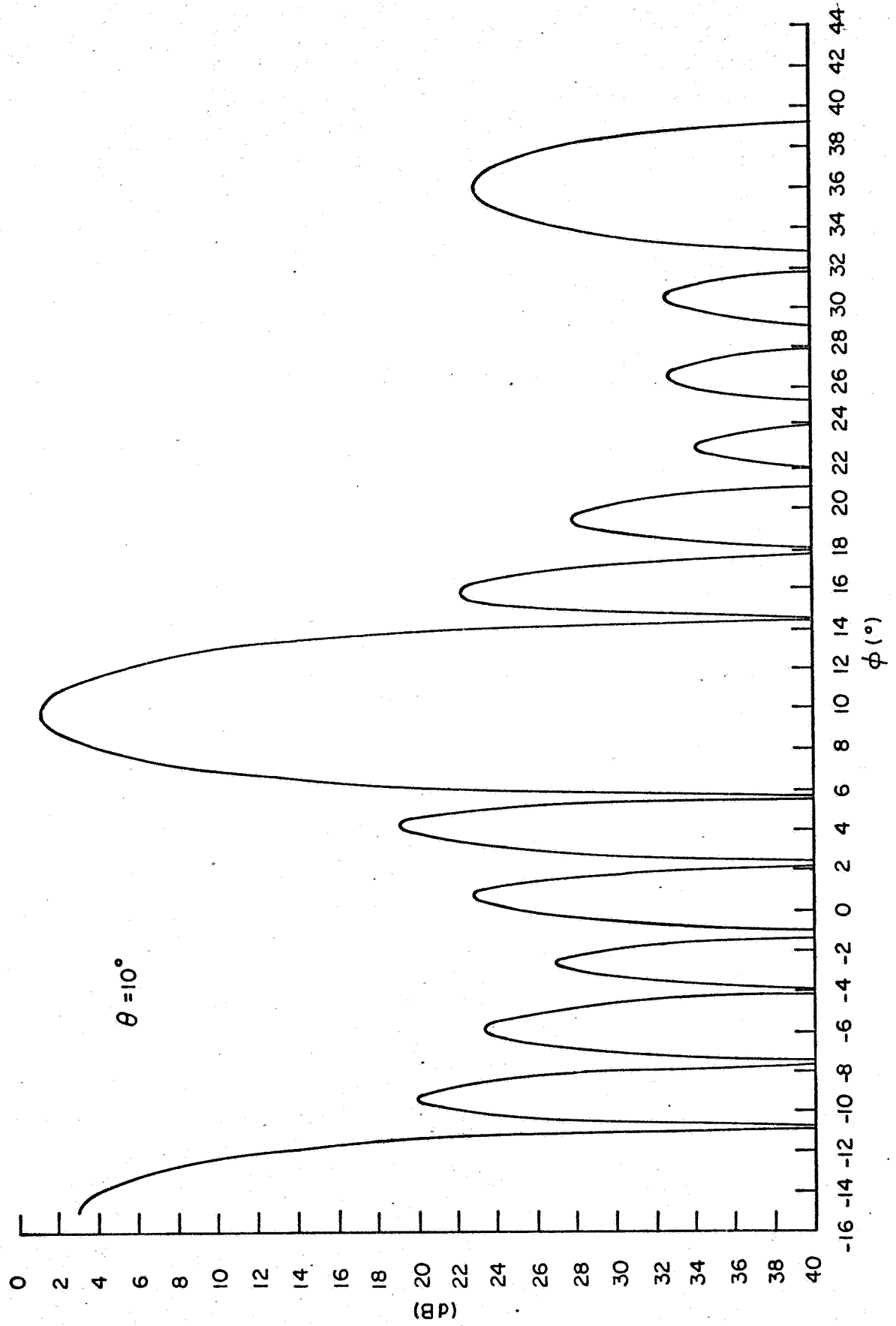


FIG. 2 - ELECTRIC FIELD CALCULATED WITH VARIATION IN AMPLITUDE TERM

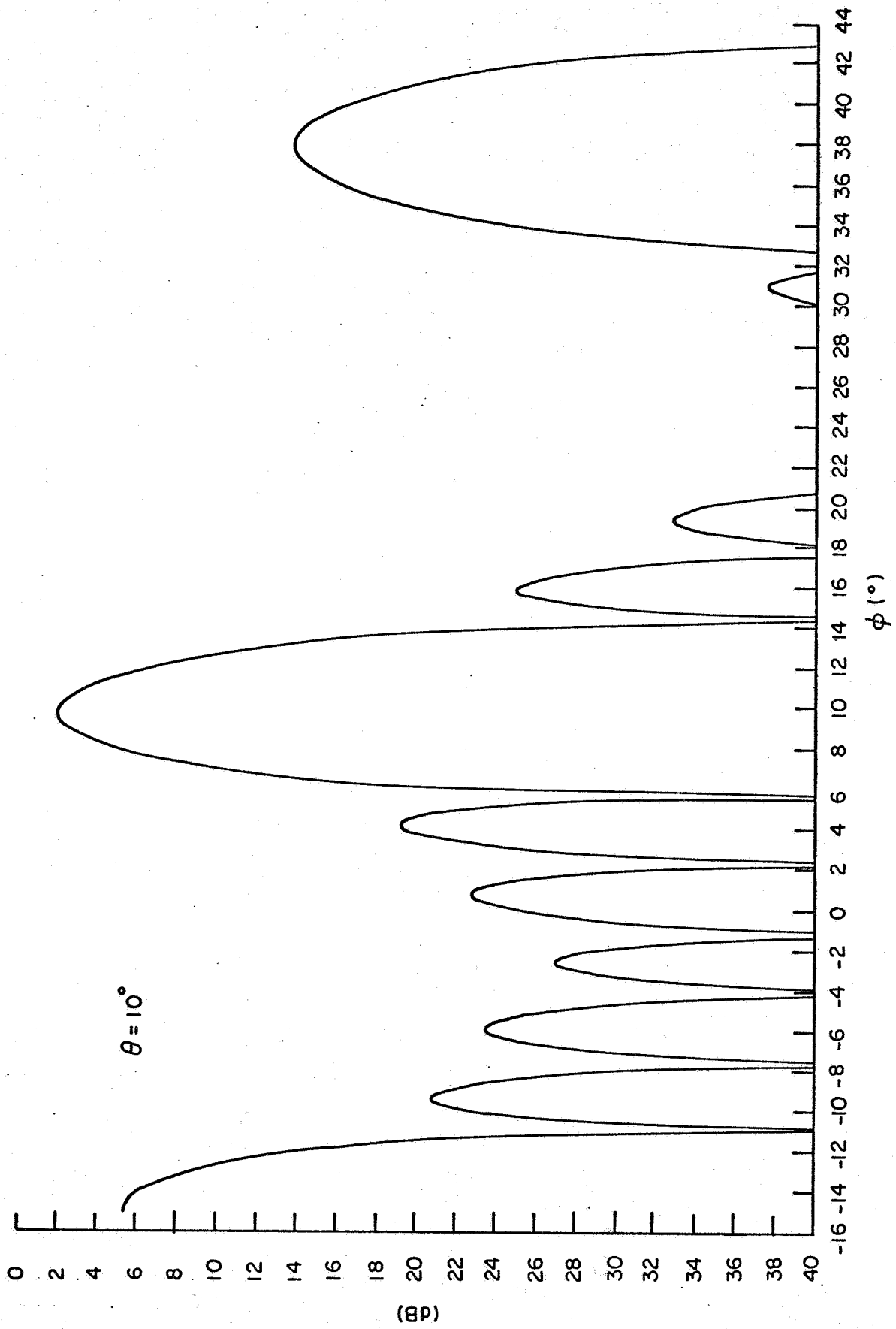


FIG.3-ELECTRIC FIELD CALCULATED WITHOUT VARIATION IN AMPLITUDE TERM

evaluated in closed form. Some data had been computed earlier using the integrated expressions, and this could now be compared with the Simpsons rule computer evaluation of the integrals. The disagreement in general was no worse than .03 dB indicating that the approximate solution of the integral is sufficiently accurate.

A summary of the most pertinent data is given in the following two tables. For the 36 patterns computed, the amplitude of the main beam and the higher first sidelobe are given. All magnitudes have been referenced to the unsteered beam with a flat phase characteristic.

	Uniform Phase	1/2 Radian Variation	1 Radian Variation
No Steering			
Main Beam	0	-.09	-.34
1st Side Lobe	-19.37	-19.45	-19.68
Steer 2°			
Main Beam	-.15	-.14	-.39
1st Side Lobe	-19.12	-19.21	-19.45
Steer 4°			
Main Beam	-.21	-.29	-.53
1st Side Lobe	-18.98	-19.07	-19.32
Steer 6°			
Main Beam	-.47	-.54	-.77
1st Side Lobe	-18.94	-19.02	-19.28
Steer 8°			
Main Beam	-.82	-.89	-1.10
1st Side Lobe	-18.99	-19.08	-19.33
Steer 10°			
Main Beam	-1.29	-1.35	-1.53
1st Side Lobe	-19.15	-19.24	-19.48

Table 1 with Variation in the Amplitude Term

	Flat Phase	1/2 Radian Variation	1 Radian Variation
No Steering			
Main Beam	0	-.24	-.90
1st Side Lobe	-19.74	-19.92	-20.51
Steer 2°			
Main Beam	-.10	-.33	-.97
1st Side Lobe	-19.24	-19.48	-20.12
Steer 4°			
Main Beam	-.38	-.59	-1.20
1st Side Lobe	-19.00	-19.24	-19.90
Steer 6°			
Main Beam	-.84	-1.02	-1.59
1st Side Lobe	-18.93	-19.17	-20.16
Steer 8°			
Main Beam	-1.49	-1.64	-2.13
1st Side Lobe	-19.05	-19.27	-19.92
Steer 10°			
Main Beam	-2.35	-2.47	-2.86
1st Side Lobe	-19.35	-19.56	-20.16

Table 2 without Variation in the Amplitude Term

2.2 Element Design and Fabrication

On the basis of the data just presented, it was decided to use horns with approximately a one-half radian phase variation. One could agree that use of the shorter horns to conserve space would only result in an additional .66 dB of loss in the worst case. However, such small losses taken at various points in the feed structure keep accumulating and the sum effect can be serious. Hence, it was felt in this case it would be better to use the extra inch of space than build more losses into the system.

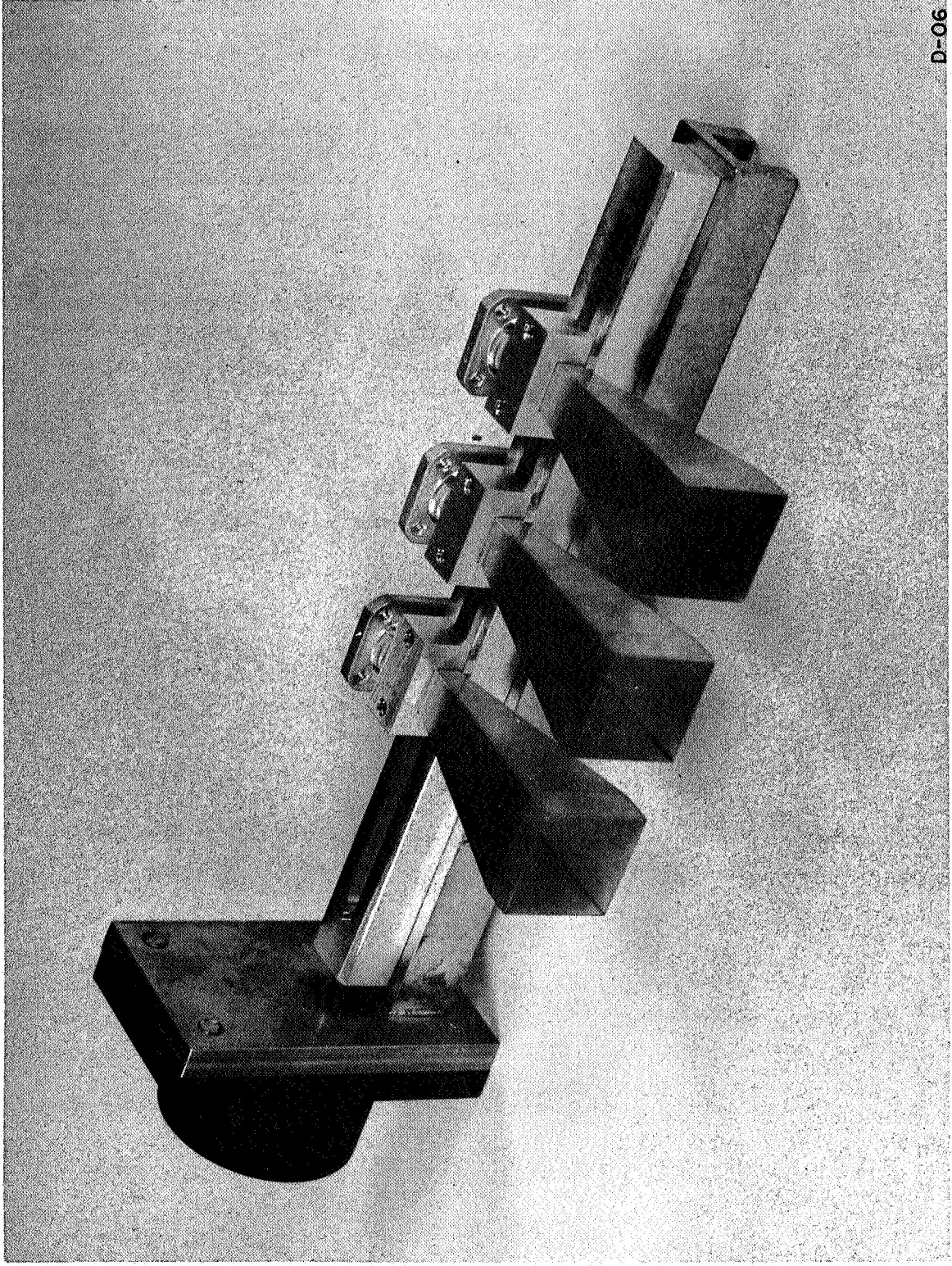
In order to stay close to the computed case, the horns were designed so as to have slightly more than the $1/2$ radian variation in one plane and slightly less in the other. It is not possible to have a square pyramidal horn on rectangular guide with equal phase centers in both planes.

At the outset, three of these horns were fabricated and pattern measurements taken to determine the effect, if any, of mutual coupling between these elements. The simplest fabrication technique for the array will be to have these horns in close contact. It was necessary first, however, to see the effect on the individual element pattern which the proximity would have before assembling the cluster of 49.

An indication that the effect of the mutual coupling should be very slight was given in a recent letter by Hamid.* Although this paper shows theoretically and experimentally that the case of zero separation is a worst case, the cross coupling between these three λ horns was still below -51 dB for this configuration. It was anticipated that this type of interaction would put a negligible perturbation on the transmitter pattern.

Figure 4 shows the first elements as they were fabricated in place on the test fixture. It can be seen here that the aperture size is only slightly larger than the standard flange for RG-96/U waveguide. Hence, when the full array of 49 horns is fabricated, the waveguide side will be virtually a solid wall of flanges with access from one side only. This places a requirement that the item to be bolted to these flanges - in this case the phase shifters - have some access from the

* M. A. K. Hamid, "Mutual Coupling Between Sectoral Horns Side By Side", IEEE Trans. on A. P., Vol. AP-15, pp. 475-477; May, 1967.



D-06

FIG. 4 - Horn Pattern Test Fixture

rear of its flange. As the phase shifters have been built in the past in the form of a solid 3/4" square block, the requirement is not met. Consultations with the phase shifter designers at Westinghouse during this period have led to an agreement that they can modify their mechanical arrangement to permit the two assemblies to be compatible.

2.3 Preliminary Test Results

The first tests performed on the elements were directed toward determining the effects, if any, of mutual coupling on the element pattern. As noted earlier, it was anticipated that these effects would be small. As a first check, the elements were mounted on the test fixture shown in Figure 4. The bracket on the end of the fixture mates with an antenna mast on the roof of the ADTEC facility. This mast permits rotation of azimuth or elevation, and is connected with automatic pattern recording equipment.

For convenience the patterns were taken with the elements in a receiving mode. The transmitter was a square pyramidal horn with approximately a five inch aperture located some 30' away. (D^2/λ for the larger aperture is roughly six feet so that far field requirements are well maintained.) Patterns were first taken with a single horn on the test fixture to determine the unperturbed element pattern. Cuts were taken in the azimuth and elevation plane on both polarizations.

Next, a second horn (terminated) was added to the fixture, and the patterns repeated as the additional horn was moved from a spacing of 1/2" away up to and including the point of contact. This procedure was then repeated with two flanking loaded horns, starting with half inch spacings and decreasing symmetrically to the point where the three horns were in contact.

Analysis of the data then showed that the only configuration having any noticeable effect was in the E-plane pattern using horizontal

polarization. Here the first sidelobe and first null were slightly altered from the single element case. The effect was not pronounced, but raised the first sidelobe about 1/2 dB and filled in the first null approximately 1 dB.

This result gave no conclusive feel as to the effect this perturbation would have on the array pattern. Hence, the next test was to use two active elements. For this case, patterns to date have been restricted to the E-plane horizontal polarization case inasmuch as it was the only one indicating a potential problem. This requires an azimuth cut of the aperture, and hence the element factor comes into play as the horns go in and out of phase in the rotation.

Element factors were calculated for the cases of two and three adjacent elements with the $16\lambda/7$ spacing which the array is planned for. The element factors were converted to dB, and the results are shown in Figures 5 and 6. These factors are for the on-axis case, i. e. no steering. The pattern of the array will then be the product of the element factor with the array factor. The measured single element pattern is reproduced in Figure 7. This is the E-plane pattern of a single element taken with no adjacent horns. The computed 2 element array factor was then applied to this measured pattern computationally and the result plotted. If the coupling effect between the two horns were negligible, the measured pattern should then agree with this hand plotted case.

The measured pattern was taken by first getting the test fixture aligned on boresight, and then phasing the two horns. The summation was accomplished by manually operating mechanical phase shifters and summing in a hybrid tee. The phasing was done using a detector on the difference port of the hybrid and adjusting the phase for a null on boresight. The detector was then moved to the sum

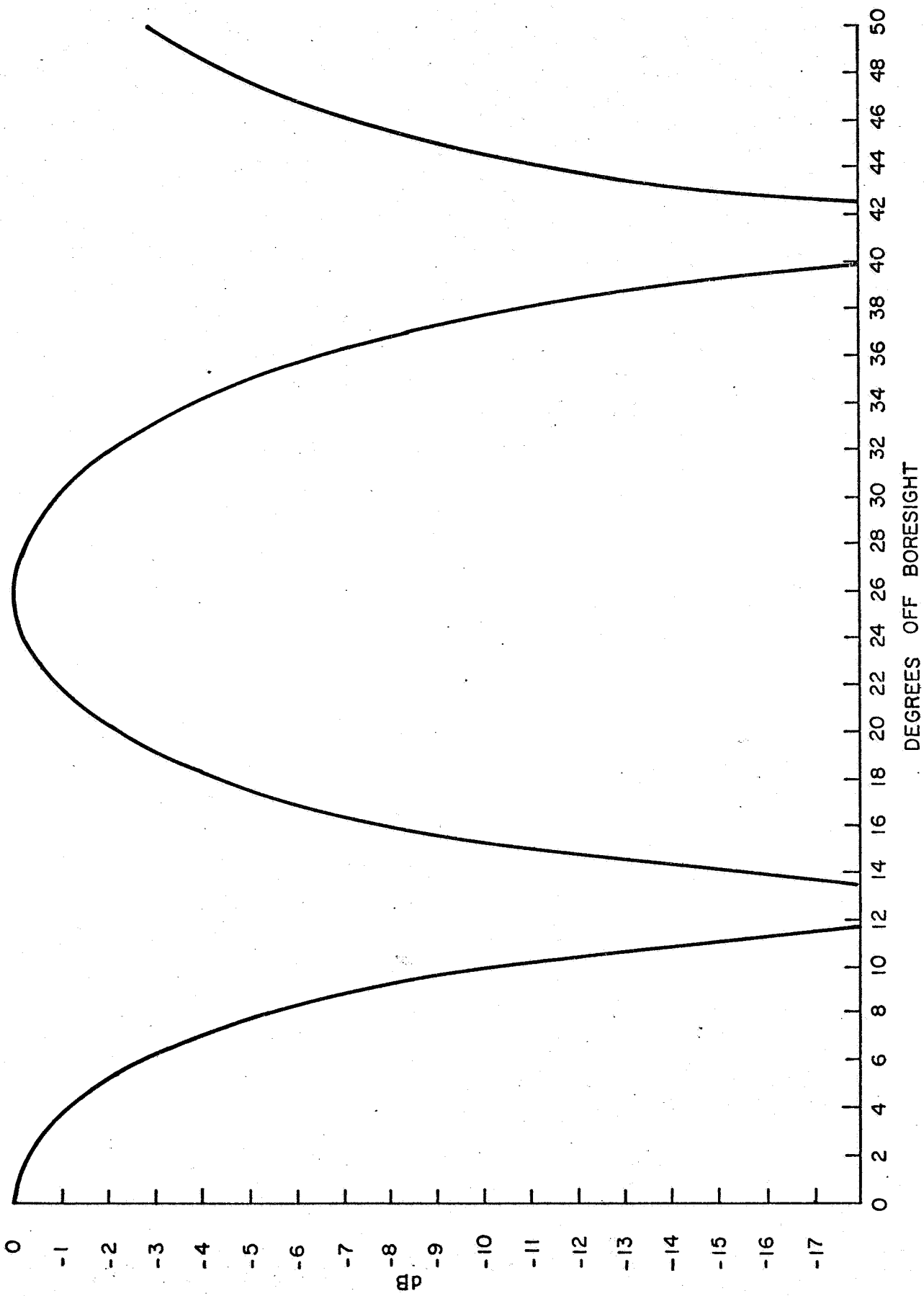


FIG. 5-ARRAY FACTOR FOR TWO ELEMENTS ON $\frac{16}{7}\lambda$ CENTERS

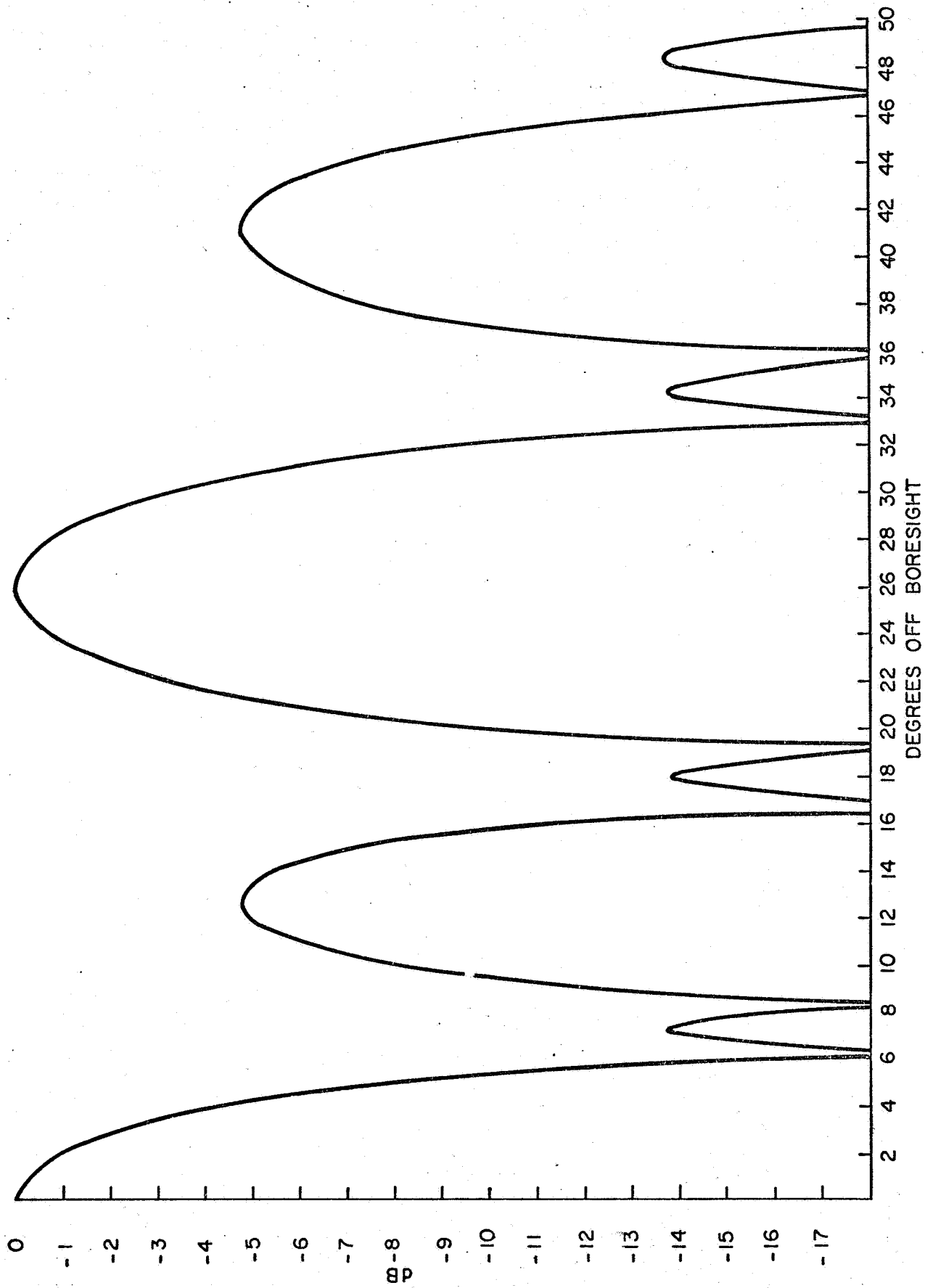


FIG. 6-ARRAY FACTOR FOR THREE ELEMENTS ON $\frac{16}{7} \lambda$ CENTERS

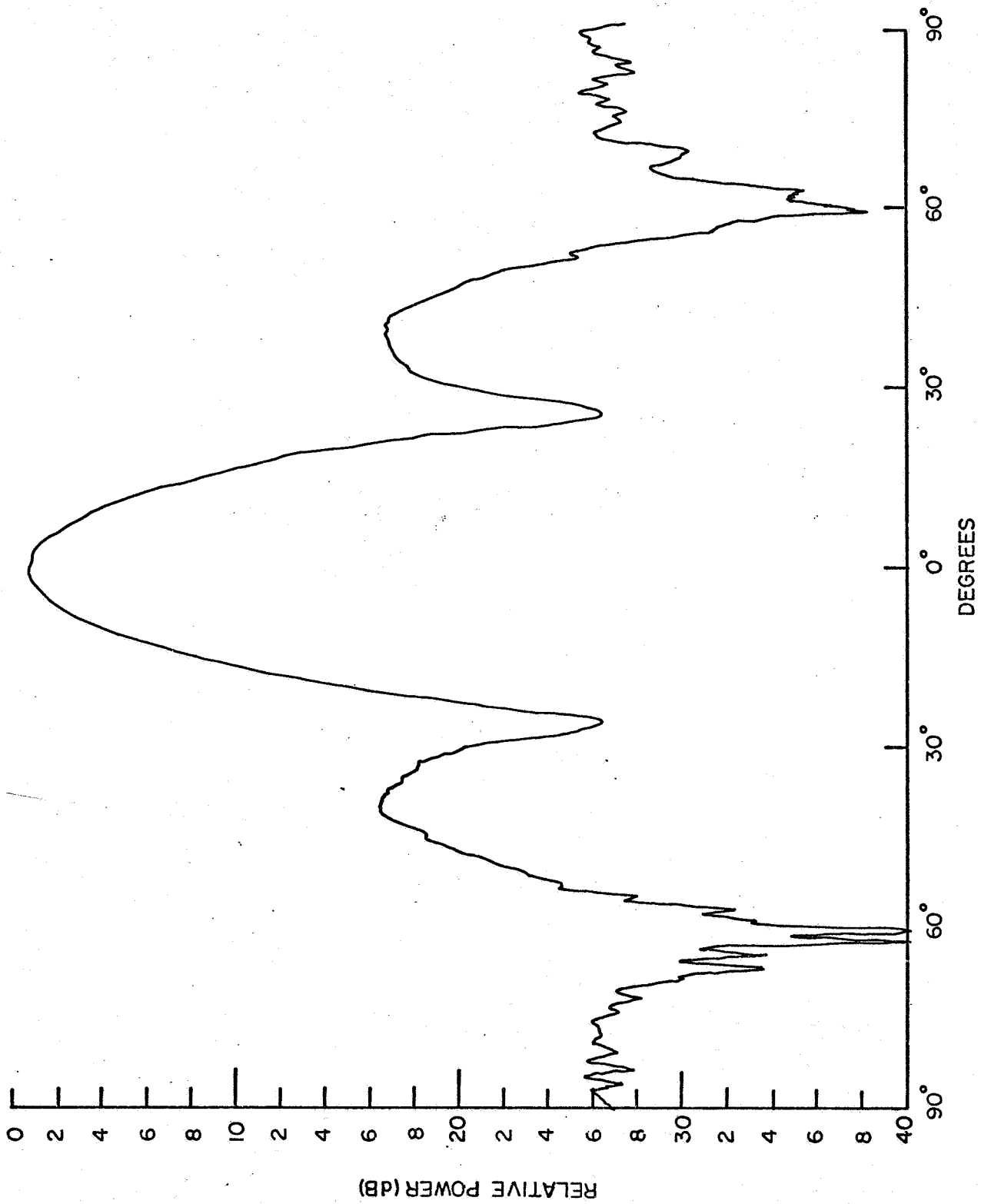


FIG. 7 - SINGLE ELEMENT PATTERN E-PLANE HORIZONTAL POLARIZATION

port and the pattern recorded.

Figure 8 shows the computed pattern based on the measured single element, and Figure 9 shows the measured pattern of the two horn pair. The agreement between computed and measured sidelobe locations and levels is excellent.

The next step was that of investigating a similar pattern when the two elements were set for 10° steering. Again this was accomplished by steering the antenna pair 10° off boresight, manually phasing for the null in the difference signal, and recording the sum signal. At the time the measurement was made it seemed possible that bad effects were being seen, for no matter how carefully the phasing was accomplished, the maximum on the measured pattern occurred at 7° . When the pattern was calculated, however, it became apparent the measurements were indeed accurate, for with only a two element array factor applied to the single element pattern the calculated peak does indeed occur at 7° . Between 7 and 10 degrees, the element pattern dominates the array factor for this simple case. The computed and measured results are shown in Figures 10 and 11. Here again, the agreement is quite good.

There is no evidence in either pattern that the mutual coupling between elements will have any serious effect on the array pattern. The nulls which in theory go to zero are filled in to a degree on the measured pattern, but this is attributable to a large extent to the fact that the hybrid tee is not a perfect summer but has finite directivity.

It was initially planned to take data summing three elements. In this case the summation becomes more complicated to instrument. On the basis of the two element data it was felt that the effort involved in repeating the process with three would not be

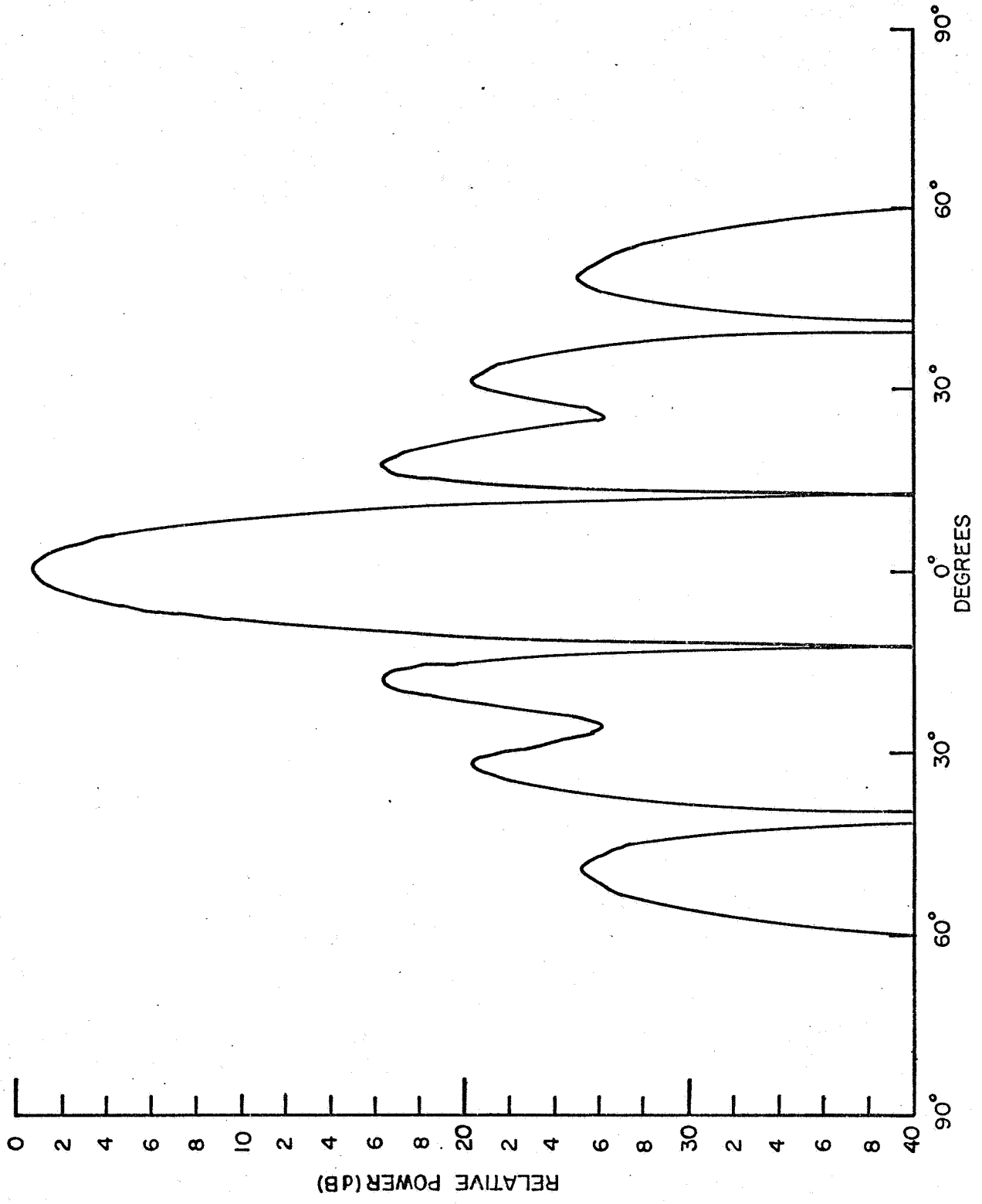


FIG. 8 - COMPUTED PATTERN; 2 ELEMENTS PHASED ON .BORESIGHT;
E-PLANE; HORIZONTAL POLARIZATION

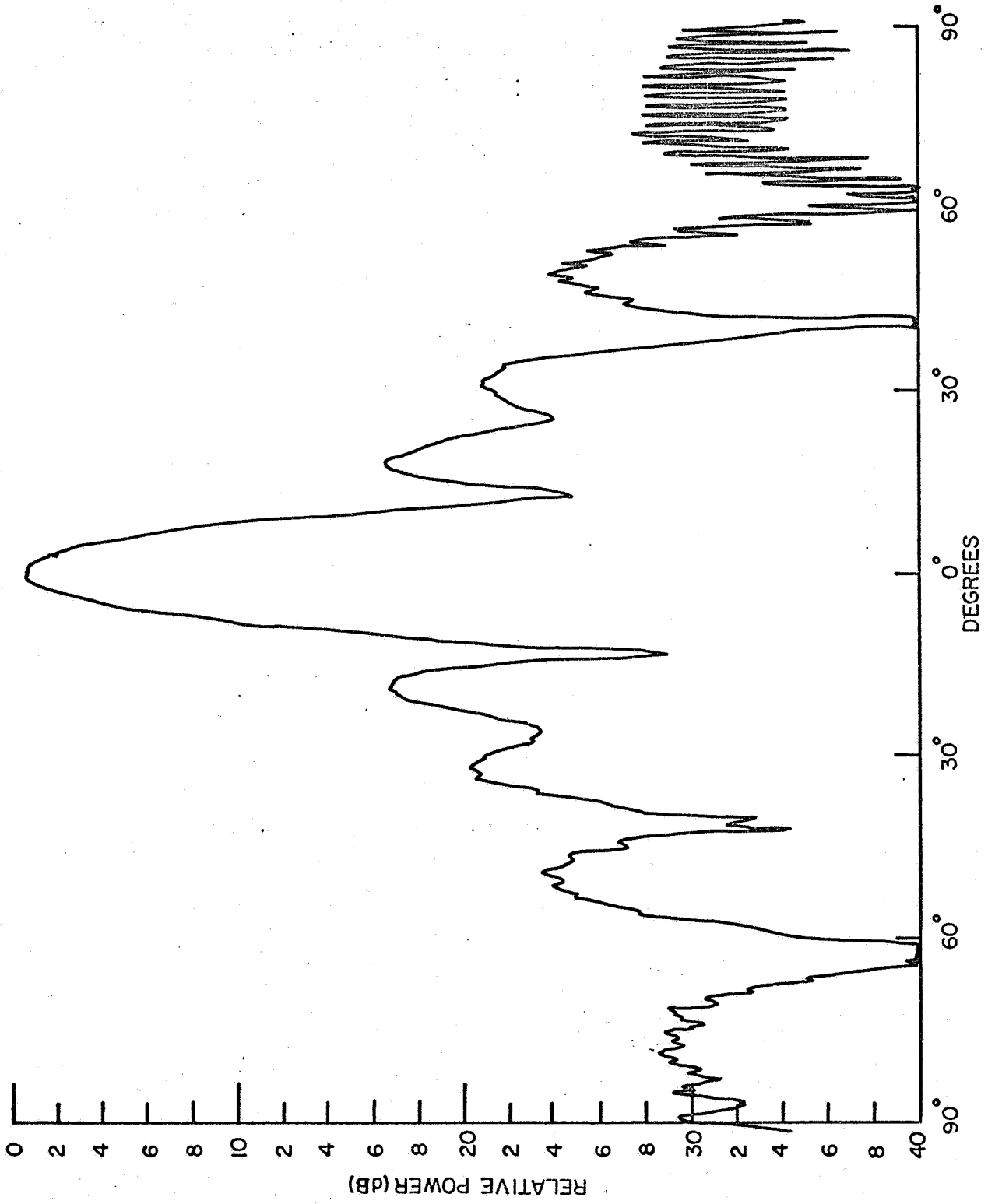


FIG.9 - MEASURED PATTERN; 2 ELEMENTS PHASED ON BORESIGHT; E-PLANE HORIZONTAL POLARIZATION

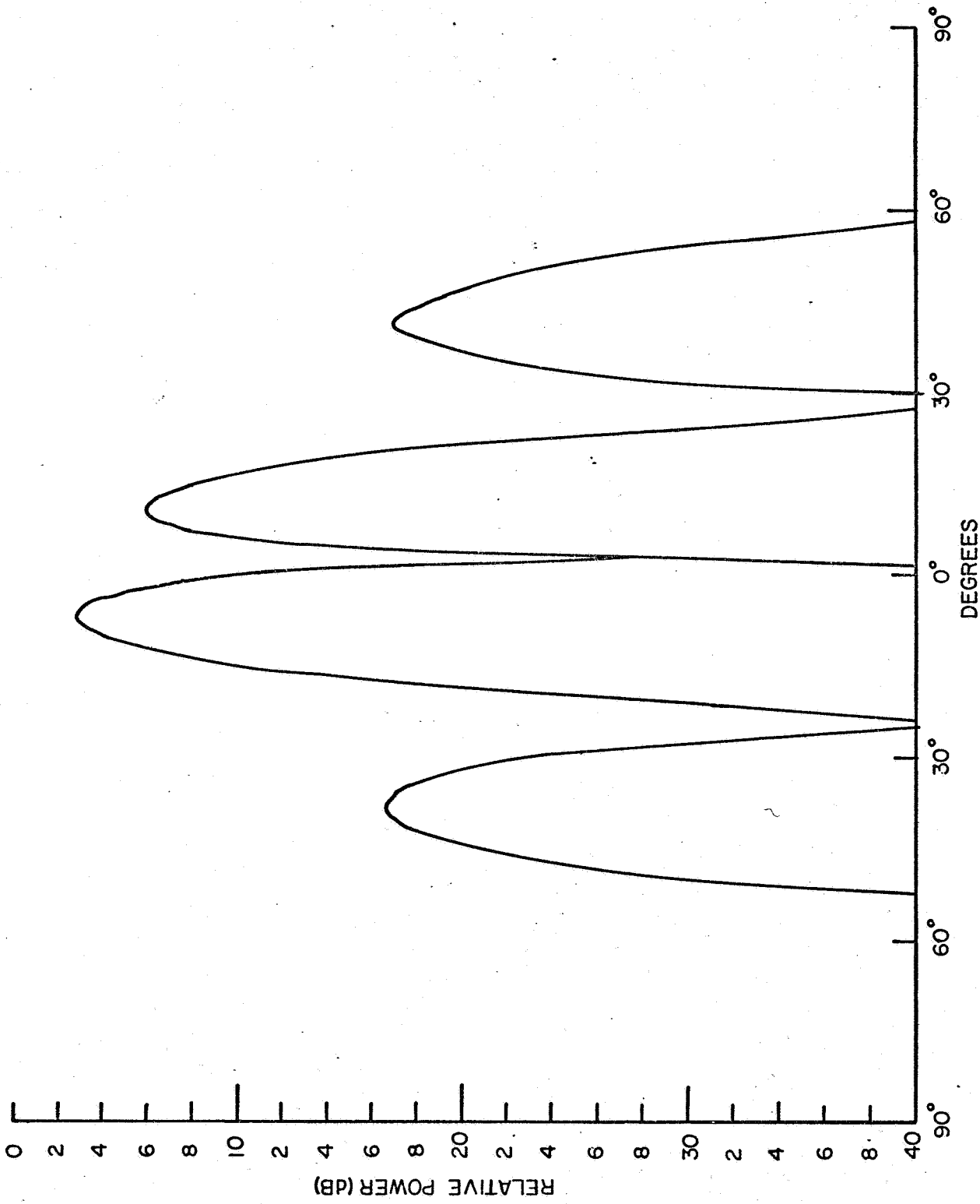


FIG.10-COMPUTED PATTERN; 2 ELEMENTS PHASED 10° OFF BORESIGHT;
E- PLANE; HORIZONTAL POLARIZATION

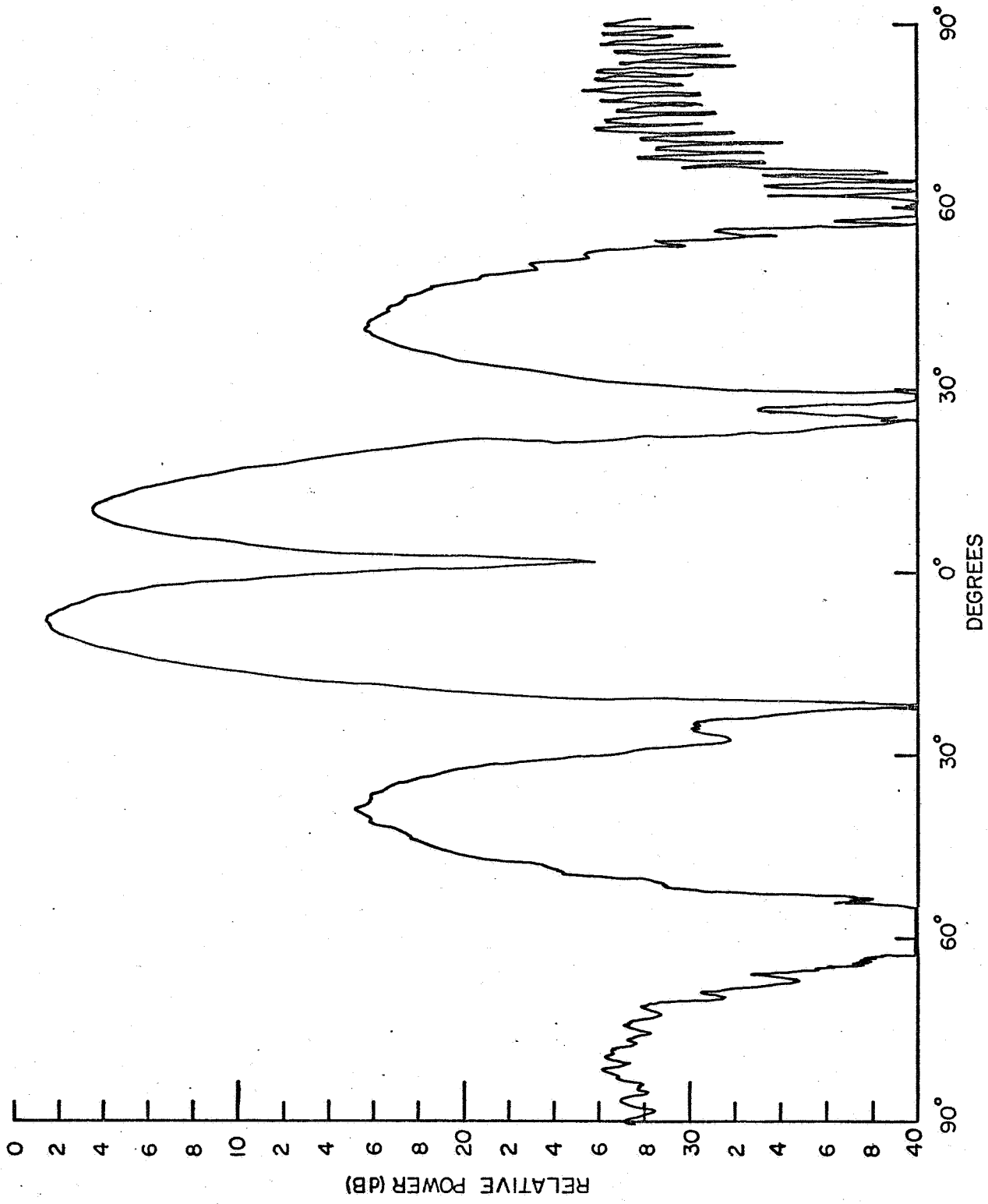


FIG.II-MEASURED PATTERN; 2 ELEMENTS PHASED 10° OFF BORESIGHT;
E-PLANE; HORIZONTAL POLARIZATION

worthwhile - one should take a larger step. Since it is almost as much work to instrument four or five elements as it is the full row of seven, and since the calculations for the seven element case have already been performed, the next experimental data will be taken using the filled row.

3. FEED SYSTEMS

3.1 Series Feed

The problems involved in the development of the coupler feed system have been resolved during this period. The previous quarterly report presented the computed values that each coupler in the series string should have, allowing for the loss at each junction. Both narrow wall and broadwall slot and iris couplers have been evaluated during this period. It has been found that the coupling coefficients in the range of 13.2 dB up to 2.9 dB were possible to achieve using slots in the broad wall of the waveguide. The required final coupling coefficient of 1.5 dB however could not be achieved in the same fashion. The problem was resolved, however, through the use of what one might call a "leaky mitered bend." The test fixture which was made is shown in Figure 12. The first data taken on this fixture were to check its operation as a conventional E-plane mitered bend. This was done by inserting a blank brass shim in the piece shown with the screws, and bolting the assembly together. The brass shim then serves as the standard mitered wall of the bend. Measurements taken over the range of 33 to 38 GHz showed the piece to have a negligible insertion loss in this configuration and a VSWR which ranged from 1.02 to 1.09.

Next, a variety of coupling holes were made up in brass shims such as the one pictured. Some of the energy then couples straight through, although most is reflected around the bend. With the irises in place, the uncompensated VSWR generally went up to about 1.5 to 1. The tuning screws, however, could always reduce this to a value of 1.02 or less.

Among the irises tested at 35 GHz, coefficients of 1.9, 1.8, 1.5, 1.25, and 1.15 dB were achieved with a matched input.

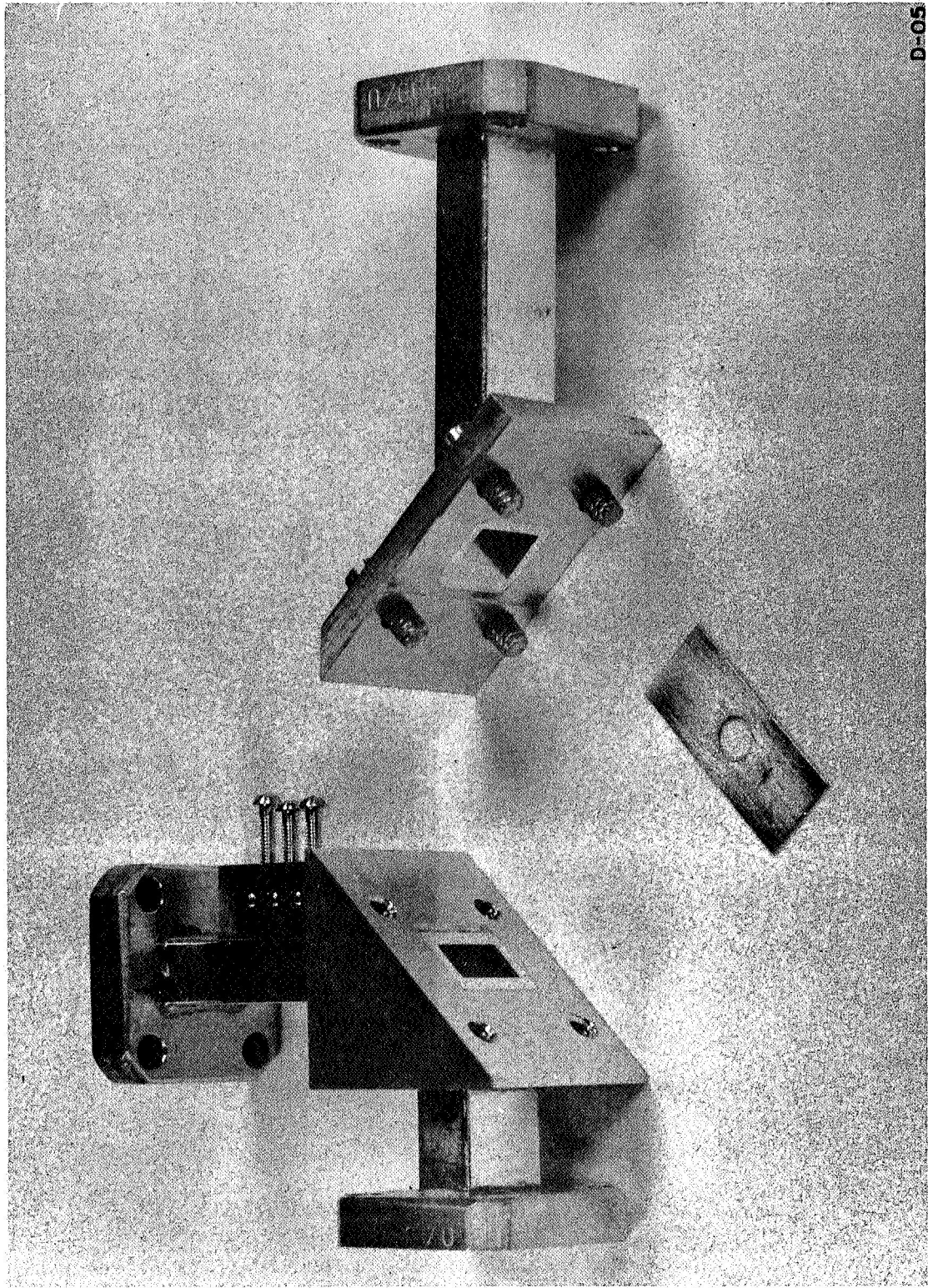


FIG. 12 - Leaky Mitered Bend

Intermediate values could also have been obtained. Hence, it seems apparent that in the final model the proper value of coupling can certainly be obtained.

Thus, to date it has been experimentally demonstrated that all the desired coupling coefficients can be achieved within the desired space limitation. The next problem to be undertaken is that of achieving them simultaneously, curing all the mutual effects, and preserving the match along one piece of waveguide which is slightly over five inches long.

The initial design of the feed structure has been completed and fabrication has begun. In the coming period, the three feed sections should be experimentally completed, and the relative phases of the outputs measured such that testing of the antenna can be undertaken when the phase shifters are received.

3.2 Optical Feed System

The alternative approach which this program will investigate is the use of an optical type of power divider. Here, one horn will be used to illuminate an egg-crate array of pyramidal horns. Experimental work on this phase will not be undertaken until the regular output array has been fabricated. This array will then be used as a tool in the experimental design of the input array.

The procedure anticipated is that the illuminating horn will be designed and tested with the grid of square horns to determine general efficiency. The distribution of power into the square grid can then be measured by checking the output of each horn at its waveguide port. From this measurement and the knowledge of the field distribution of the illuminating horn inference can be made concerning the changes in aperture sizes which will be necessary to produce the desired illumination taper for the feed grid.

4. PHASE SHIFTERS

In the coming period, we will be working closely with the personnel at Westinghouse while the latching ferrite phase shifters are being produced to assure that the interfaces at the feed system and the horn array are properly established. For this preliminary model only one driver is being built. No dynamic steering tests are contemplated. For the pattern testing, data will be taken at pre-selected steering angles. The required states for each phase shifter will be calculated. Since these are four bit devices, each phase shifter will have five control wires associated with it. These leads will be brought from the antenna mast to the control area to a 5 gang, 14 position switch. The operator can then set each phase shifter in turn from the one driver and record the pattern.

The prototype models of the phase shifters are using an improved nickel-zinc ferrite which has a figure of merit of $375^{\circ}/\text{dB}$. In the actual four bit package, due to losses incurred at the discontinuities and in the transformer sections, the loss is approximately 1.25 dB.

In the development work now going on at 75 GHz, it is anticipated that the phase shift of $200^{\circ}/\text{inch}$ can be achieved as it was at 35 GHz. With the present geometry, however, only $108^{\circ}/\text{inch}$ has been achieved so far, which of course leads to a much lossier device. If changes in the toroid structure achieve the desired increase in activity, a figure of merit of about $180^{\circ}/\text{dB}$ could be obtained.

At 94 GHz, the situation becomes even worse. The toroids become extremely difficult to fabricate and the losses due to lack of geometry optimization can become larger. The theoretically achievable figure of merit also decreases. The net result is that the present prediction for a 94 GHz phase shifter is that it would probably be about a 4 dB insertion loss device. This does not bode well for scaling the

present antenna design to the 94 GHz range.

Because of this consideration, possible alternative methods will be examined during the remainder of the contract. Earlier work in the study phase of this program has already indicated that lacking phase shifters in the r. f. portion of the antenna, the best general approach would involve some type of retrodirective technique. Here the critical components become the up and down converters. In the coming periods these will be examined in detail to provide a basis for a valid comparison with the rather high loss phase shifter approach.

21

5 VARACTOR MULTIPLIERS

Attempts have been made in this period to collect data on phase variation through varactor harmonic generators as a function of phase and amplitude variations at the fundamental. To this end a phase bridge has been set up. At 17.5 GHz, the available power is split through the use of a directional coupler and applied to two multipliers which have been set up to be nearly identical. The loop is then closed by bringing the 35 GHz power to opposite ends of a slotted line. There is adequate harmonic power available such that this can be done through 30 dB of attenuation on either side of the slotted line thereby achieving isolation between the doubler outputs.

In one arm at the fundamental, there is included a rotary vane attenuator and a phase shifter. Due to the difficulty in locating a direct reading phase shifter which had a constant insertion loss, a substitute device has been fabricated and checked in this period. This unit consists of a sidewall hybrid with a pair of ganged tunable short circuits. The 1/2" micrometer drive which was used then permits a change in excess of a guide wavelength through the device. The insertion loss of this phase shifter measures about 0.2 dB and the input VSWR ranges from 1.02 to 1.25 as the positions of the short circuits are varied. Hence, the phase shifter is a useful device for the measurements.

In the early stages of the measurement attempts were made to get the two multipliers operating in a nearly identical fashion as regards efficiency, input VSWR, etc. After considerable adjustment, one was made to have an efficiency of slightly over 50% as measured with a square wave modulated input (250 mW peak input - 125 mW average). The other was 5% less in efficiency, but it was felt that this would be close enough since both units were working well.

The two multipliers were then set up such that the harmonic

output fed a phase bridge network. The input power to the two was then lowered by use of a single precision attenuator preceding the fundamental power divider. This was done to simulate the action which might occur in a harmonic transmitting array should the primary source begin to lose power.

The results obtained were not terribly encouraging for this type of approach to a transmitting array. The change in the relative phase between the two signals is shown in Figure 13. With a 5 dB change in the input signal, the relative phase variation exceeds a half wavelength.

In an effort to gain more insight into the causes, the efficiencies of the multipliers were measured individually as a function of input power. These results are shown in Figure 14. The more efficient multiplier maintained its efficiency well over almost 3 dB input variation before rolling off. The other multiplier, however, fell off immediately and rather erratically. The abrupt change between 2 and $2\frac{1}{2}$ dB correlates well with the rapid change of phase difference in Figure 13. There is nothing else however which can readily explain the steady drift in the relative phase through the rest of the plot. If the path lengths to the point of the phase measurement were greatly different and the tube frequency were changing in spite of the presence of the isolator, the phase departure could be explained from this point of view. Efforts were made, however, to keep these line lengths fairly close, and if one theorizes a path difference of $10''$, or about $25\lambda_g$ at 35 GHz (which certainly does not exist here) then the tube frequency would have to shift 1 part in 50 or some 350 MHz to cause this phase difference. Although the tube frequency was not monitored during the measurement, much of the data was repeated, and it is unlikely that klystron changes would be that large and also repeatable.

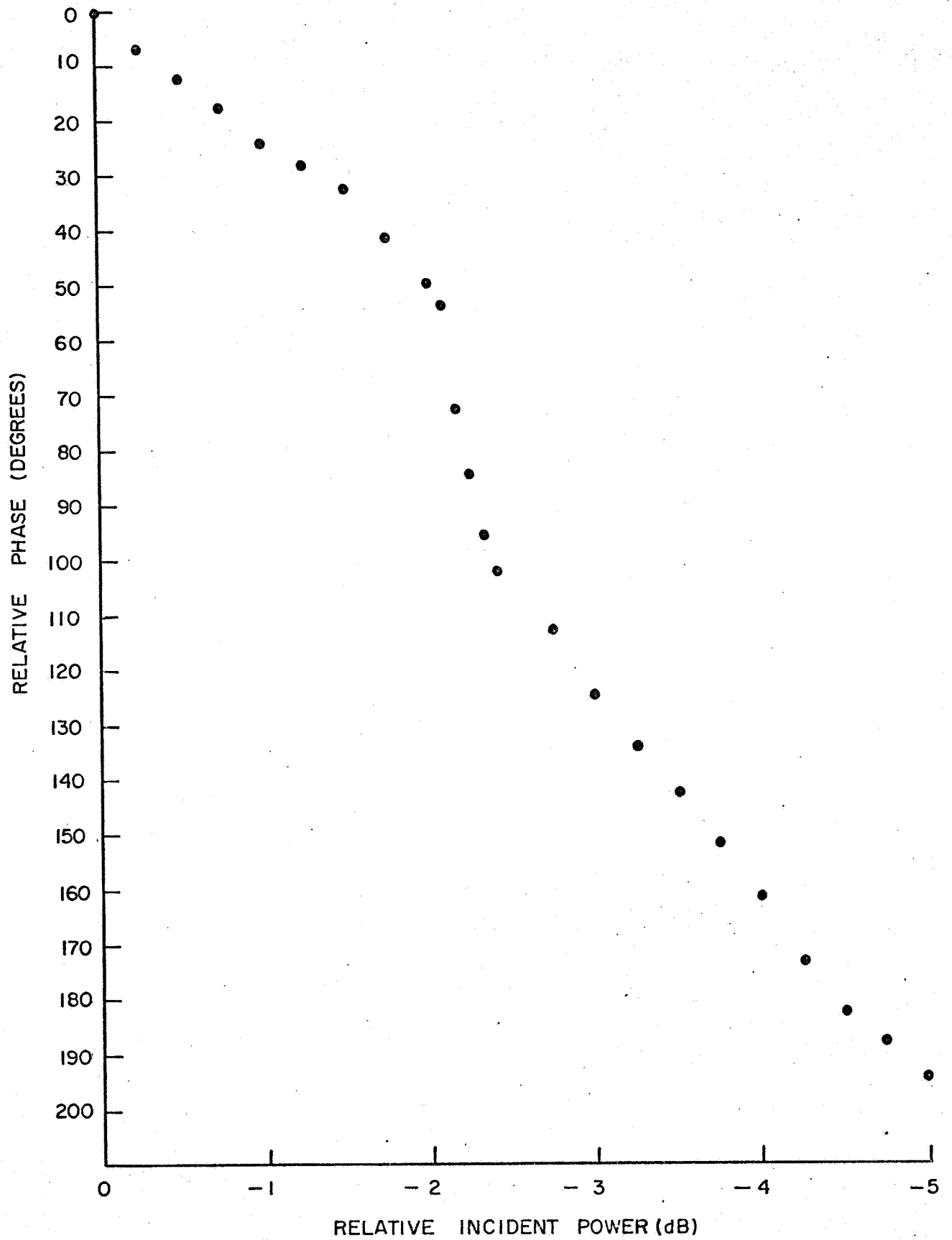


FIG13-PHASE DIFFERENCE IN OUTPUT OF TWO MULTIPLIERS

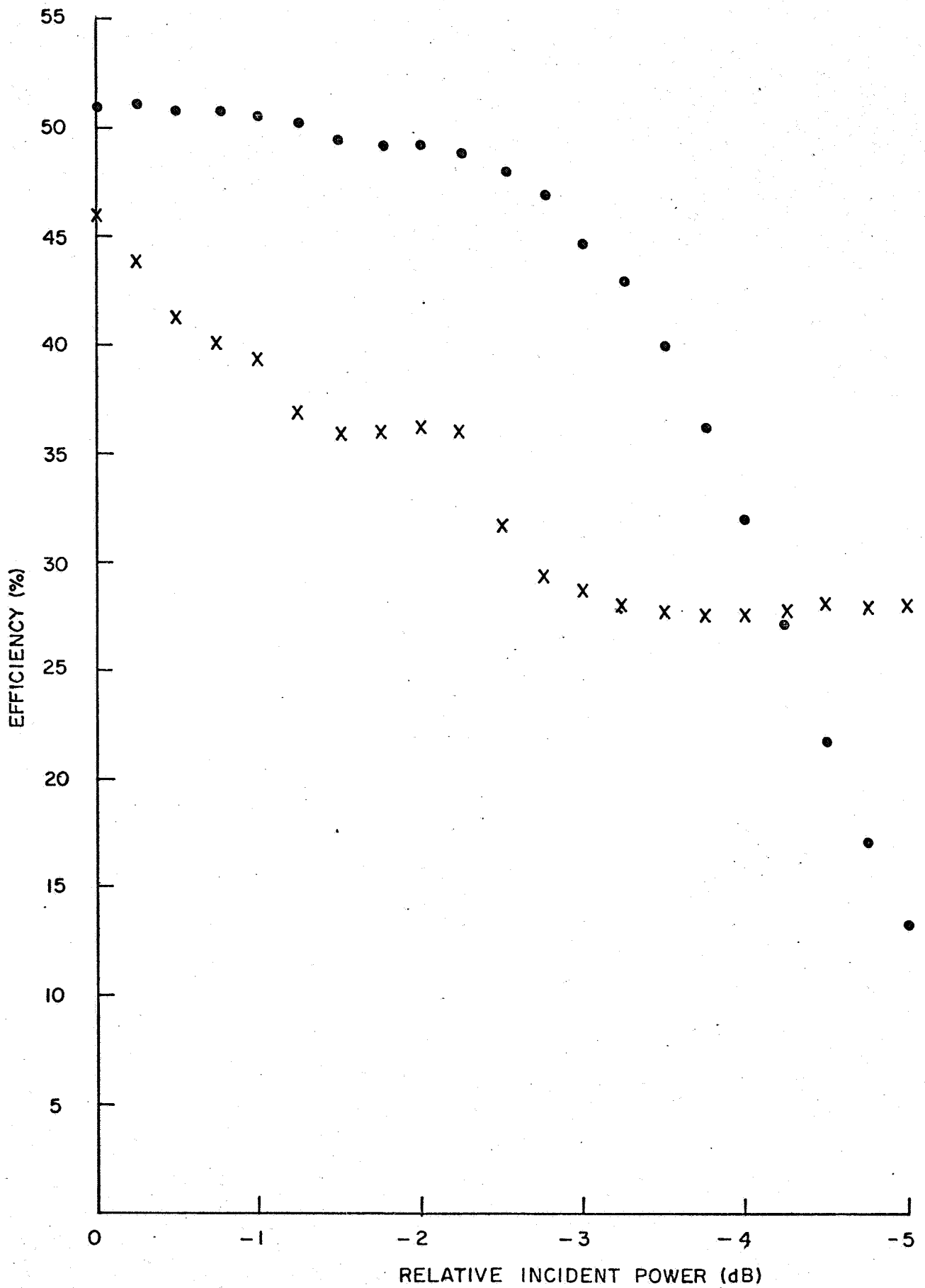


FIG.14-EFFICIENCY CHARACTERISTICS OF TWO MULTIPLIERS

31

The next test planned is to attempt to match the multiplier efficiency curves over the range of input powers, and then repeat the phase characteristic measurements.

6. NEW TECHNOLOGY

During the period covered by this report there have been no inventions or discoveries which may be considered under the New Technology clause of the contract.

5

7. PROGRAM FOR THE NEXT INTERVAL

During the next quarter, work will be pursued in several areas leading to the assembly of the feasibility model of the antenna.

Fabrication and test of the seven coupler feed system should be completed in this interval, and the output horn array will be assembled and ready for test.

The antenna testing program will be thoroughly planned and all equipment, test fixtures, etc., necessary to implement the testing will be procured or fabricated.

Work will continue on examination of the phase characteristics of the harmonic generators.

A theoretical investigation of retrodirective techniques for a 94 GHz system will be pursued to determine the critical components and establish specifications on their performance.